Research in Electromagnetic Scattering

Final report for Contract # F49620-97-C-0017 submitted to the Air Force Office of Scientific Research

by

A.J. Devaney Associates, Inc.
295 Huntington Ave., Suite 208
Boston, MA 02115

Abstract

This document constitutes a final report for our research in electromagnetic scattering during 1997. The technical research accomplishments divide conveniently into the areas of time-domain electromagnetics, high-frequency diffraction, and surface integral equations. As principal investigator, Dr. Arthur D. Yaghjian carried out the major portion of the research, and coordinated his efforts with those of T.B. Hansen and R.A. Shore of Rome Laboratory, R.A. Albanese of Brooks AFB, S.W. Lee of DEMACO, and R. Tolimieri, M. An and A.J. Devaney of A.J. Devaney Associates.

1 Technical Summary of Accomplishments

In 1997 our research accomplishments in electromagnetic scattering divide conveniently into three main areas:

- Time-Domain Electromagnetics
- High-Frequency Diffraction
- Surface Integral Equations.

1.1 Time-Domain Electromagnetics

Plane-Wave Theory of Time-Domain Fields

In the area of time-domain electromagnetics, Dr. Arthur D. Yaghjian and Dr. Thorkild B. Hansen have been working together to develop the "plane-wave theory of time-domain fields," and to apply this theory to the near-field scanning of antennas and scatterers. Previously, near-field measurement techniques had been formulated only for antennas and scatterers

operating over a narrow frequency band, that is, only in the frequency domain. The new time-domain formulation allows powerful near-field measurement techniques to be extended to pulsed radiators (antennas or scatterers) operating over arbitrarily wide bandwidths. This time-domain near-field measurement formulation was published in the IEEE Transactions on Antennas and Propagation [1] and received the 1995 Schelkunoff Prize Paper Award.

During 1997, Yaghjian and Hansen expanded and refined their "plane-wave theory of time-domain fields," and completed about 90% of a book under this title [2] scheduled to be published by the IEEE/Oxford University Press in 1998. Numerous additions and improvements were made to the theory. For example, Yaghjian found a direct method of deriving the dispersion relations for general electromagnetic materials that reveals the natural sufficient conditions on the constitutive parameters required for the validity of the dispersion relations. This derivation is given here in Appendix A.

An invited paper on the subject of time-domain far fields was submitted to Amerem-96, and this year an expanded version of the paper was published as a book chapter [3]. Recently, Yaghjian has been invited by the special-issues editor of the Proceedings of the IEEE to submit a review article on time-domain near-field scanning. He has also been invited to submit a paper on ultra-wideband, short-pulse electromagnetics to Euroem-98, to be held in Israel.

During the year we have assisted Analytic Designs (Columbus, OH) in their implementation of planar near-field measurements in the time domain. We have also been asked by Satimo, Inc. (Acworth, GA) and Supelect (Paris, France) to work with them in their combined effort to design a time-domain spherical near-field measurement system. In addition, the members of the SBIR evaluation committee at Rome Laboratory chose "Time-Domain Near-Field Measurements" as their top priority Phase II SBIR topic.

The table of contents of the Hansen and Yaghjian book are given in Appendix B. Final drafts of all but chapter 1 and sections 2.3-2.4 of the book have been completed. As part of the effort to develop and document the plane-wave theory of time-domain fields, Yaghjian and Hansen, along with Professor A.J. Devaney, discovered and published as an IEEE-APS Letter a profoundly simple method, using plane-wave spectra, for determining the position, size and shape of the minimum possible source region of a specified far-field pattern [4]. (The editor of the IEEE Transactions on Antennas and Propagation has asked us to submit a full-length article on this subject in the future.) The theory and application of this method, which is outlined in Appendix C, for determining the minimum source region, and the limits it gives for the smallest possible sizes of antennas that can radiate specified far-field patterns, provide antenna engineers with a new set of practical design tools.

Trajectories and Fields of Bound and Unbound Charges

The 1992 book [5] by Yaghjian has received notable acclaim by the physics community. For example, Professor Emeritus, Fritz Rohrlich of Syracuse University, considered by many physicists as the foremost expert on the classical equations of motion for charged particles,

writes

> "This is a remarkable book. Arthur Yaghjian is by training and profession an electrical engineer; but he has a deep interest in fundamental questions usually reserved for physicists. Working largely in isolation he has studied the relevant papers of an enormous literature accumulated over a century. The result is a fresh and novel approach to old problems and to their solution.
>
> Physicists since Lorentz have looked at the problem of the equations of motion of a charged object primarily as a problem for the description of a fundamental particle, typically an electron. Yaghjian considers a macroscopic object, a spherical insulator with a surface charge. He was therefore not tempted to take the point limit, and he thus avoided the pitfalls that have misguided research in this field since Dirac's famous paper of 1938.
>
> Perhaps the author's greatest achievement was the discovery that one does not need to invoke quantum mechanics and the correspondence principle in order to exclude the unphysical solutions (runaway and pre-acceleration solutions). Rather, as he discovered, the derivation of the classical equations of motion from the Maxwell-Lorentz equations is invalid when the time rate of change of the dynamical variables is too large (even in the relativistic case). Therefore, solutions that show such behavior are inconsistent consequences. The classical theory is thus shown to be physically consistent by itself. It is embarrassing—to say the least—that this observation had not been made before.
>
> This work is an apt tribute to the centennial of Lorentz's seminal paper of 1892 in which he first proposed the Lorentz force equation."

The "physically consistent" classical equation of motion (to use the terminology of Rohrlich) derived by Yaghjian can be applied to the PIC problem. When an electron is accelerated by an incoming electromagnetic pulse, the electron experiences a "radiation reaction" force in addition to the externally applied force. In 1997 we began work looking into the version of the Lorentz-Abraham-Dirac equation of motion derived by Yaghjian [5, eq. 8.76] for an accelerated charged particle

$$F^i_{ext} = mc^2 \frac{du^i}{ds} - \frac{e^2}{6\pi\epsilon_0}\eta(s)\left(\frac{d^2u^i}{ds^2} + u^i \frac{du_j}{ds}\frac{du^j}{ds}\right). \tag{1}$$

In actual application, we used the three-vector form of the equation of motion corresponding to the four-vector equation (1), namely

$$\mathbf{F}_{ext}(t) = m\frac{d(\gamma\mathbf{u})}{dt} - \frac{e^2}{6\pi\epsilon_0 c^3}\eta(t)\left\{\frac{d}{dt}\left[\gamma^2\dot{\mathbf{u}} + \frac{\gamma^4}{c^2}(\mathbf{u}\cdot\dot{\mathbf{u}})\mathbf{u}\right] - \frac{\gamma^4}{c^2}\left[|\dot{\mathbf{u}}|^2 + \frac{\gamma^2}{c^2}(\mathbf{u}\cdot\dot{\mathbf{u}})^2\right]\mathbf{u}\right\} \tag{2}$$

where $\mathbf{u}$, e and m are the velocity, charge and mass of the particle. Of course, t is the time, c is the speed of light, ϵ_0 is the permittivity of free space, $\mathbf{F}_{ext}(t)$ is the externally applied force, and $\gamma = (1 - u^2/c^2)^{-\frac{1}{2}}$. The force is applied at $t = 0$ and $\eta(t)$ is a function that increases monotonically from a value of zero to a value of unity in the time it takes light to traverse the diameter of the charged particle. In other words, $\eta(t)$ is close to a unit step function. It is this function $\eta(s)$ in (1) or $\eta(t)$ in (2) that had been previously overlooked and that Yaghjian found in his careful derivation of (1) and (2). This unobtrusive function completely eliminates the noncausal pre-acceleration that has plagued the original equations of motion ever since they were derived by Lorentz and Abraham about 100 years ago.

Although (2) is a rather complicated equation of motion, our preliminary work with particles confined to rectilinear motion shows that closed-form solutions are indeed possible. In particular, for the velocity $\mathbf{u}$ in the x direction, that is, $\mathbf{u} = u\hat{\mathbf{x}}$, we can find a general solution to (2) by making the change of variables

$$\sinh(\mathcal{V}/c) = c\gamma u \ , \quad d\tau = dt/\gamma \tag{3}$$

with

$$\gamma = \left(1 - u^2/c^2\right)^{-\frac{1}{2}} = \cosh(\mathcal{V}/c) \tag{4}$$

to convert (2) to

$$F_{ext}(\tau) = m\mathcal{V}'(\tau) - \frac{e^2}{6\pi\epsilon_0 c^3}\eta(\tau)\mathcal{V}''(\tau). \tag{5}$$

Equation (5) is a first order linear differential equation for $\mathcal{V}'(\tau)$. Its solution for all τ is given by

$$\mathcal{V}'(\tau) = \begin{cases} 0 \ , & \tau < 0 \\ \dfrac{-1}{m}\displaystyle\int_\tau^\infty F_{ext}(\tau')\frac{d}{d\tau'}\left[e^{-\frac{6\pi\epsilon_0 mc^3}{e^2}\int_\tau^{\tau'}\frac{d\tau''}{\eta(\tau'')}}\right]d\tau' \ , & \tau \geq 0 \end{cases} \tag{6}$$

where the external force is applied at $\tau = 0$ and is zero for $\tau < 0$. Integration of (6) over time produces the solution for the velocity of the charge that is zero for $\tau < 0$ and continuous for all τ, even across $\tau = 0$, as long as $F_{ext}(\tau)$ is continuous or has a finite jump across $\tau = 0$. In other words, the inclusion of the η function in the equation of motion has eliminated the pre-acceleration from the solution to the original equation of motion without introducing false discontinuities in velocity across $\tau = 0$ or spurious delta functions and their derivatives at $\tau = 0$.

1.2 High-Frequency Diffraction

In the area of high-frequency diffraction, Dr. Yaghjian has been the principal investigator during the past ten years responsible for the development of incremental length diffraction coefficients (ILDC's) that have been incorporated into production computer codes delivered to

the Air Force. This highly successful work began with his discovery that three-dimensional (3-D) ILDC's could be found directly from the two-dimensional (2-D) far fields of planar canonical scatterers [6]. Shore and Yaghjian immediately applied this discovery to finding ILDC's for cracks and ridges in metal surfaces, and this led to the first accurate prediction of cross polarized fields from reflector antennas with cracks between their panels [7]. Subsequently, ILDC's were found for truncated wedges [8], and both the truncated-wedge and crack-ridge ILDC's have been included in the Air Force codes for computing scattering from large bodies. (The truncated-wedge work won an IEEE Best Paper Award at the 1996 IEEE International Symposium on Antennas and Propagation.)

Moreover, Yaghjian has derived a theorem that removes the planar restriction on 2-D canonical scatterers used to find 3-D ILDC's. With this restriction removed, he has been able to derived (in 1996 and 1997) the first shadow-boundary ILDC's that can be used to significantly enhance the accuracy of bistatic as well as monostatic scattering computed from physical optics (PO) codes. These shadow-boundary ILDC's can be written in the form

$$d\boldsymbol{E}_{SB}(r',\theta,\phi) = d\boldsymbol{E}^{e}_{TM}(r',\theta,\phi) + d\boldsymbol{E}^{m}_{TM}(r',\theta,\phi) + d\boldsymbol{E}^{e}_{TE}(r',\theta,\phi) + d\boldsymbol{E}^{m}_{TE}(r',\theta,\phi) \tag{7}$$

where

$$d\boldsymbol{E}^{e}_{TM} = dz'\frac{C}{C_0}E^{e,TM}_{\theta_0^\pi}(\rho',\alpha,z;\theta_0)\frac{\sin\theta}{\sin\theta_0}\hat{\boldsymbol{\theta}} \tag{8}$$

$$d\boldsymbol{E}^{m}_{TM} = dz'\frac{CE^{m,TM}_{\theta_0^\pi}(\rho',\alpha,z;\theta_0)}{C_0\sin\alpha}\left[\sin\phi\hat{\boldsymbol{\theta}} + F(\phi,\theta,\theta_0,t)\hat{\boldsymbol{\phi}}\right] \tag{9}$$

$$d\boldsymbol{E}^{e}_{TE} = dz'\frac{C}{C_0}\left\{\frac{E^{e,TE}_{\phi}(\rho',\alpha,z;\theta_0)}{\sin\alpha}\left[\sin\phi\hat{\boldsymbol{\phi}} - F(\phi,\theta,\theta_0,t)\hat{\boldsymbol{\theta}}\right] + E^{e,TE}_{\theta_0^\pi}(\rho',\alpha,z;\theta_0)\frac{\sin\theta}{\sin\theta_0}\hat{\boldsymbol{\theta}}\right\} \tag{10}$$

$$d\boldsymbol{E}^{m}_{TE} = dz'\frac{C}{C_0}\left\{\frac{E^{m,TE}_{\theta_0^\pi}(\rho',\alpha,z;\theta_0)}{\sin\alpha}\left[\sin\phi\hat{\boldsymbol{\theta}} + F(\phi,\theta,\theta_0,t)\hat{\boldsymbol{\phi}}\right] + E^{m,TE}_{\phi}(\rho',\alpha,z;\theta_0)\frac{\sin\theta}{\sin\theta_0}\hat{\boldsymbol{\phi}}\right\} \tag{11}$$

with

$$F(\phi,\theta,\theta_0,t) = \cos\phi\cos\theta + \frac{t\sin\theta\cos\theta_0}{\sin\theta_0}\,.$$

The TM and TE shadow-boundary electric fields required on the right hand sides of (8)-(11) are given in [9]. Dr. R.A. Shore of Rome Laboratory tested these ILDC's by applying them to compute the high-frequency scattering from a perfectly conducting sphere of radius a

illuminated by a plane wave. The corrections computed from the incremental fields were added to the PO fields of the sphere, and the results are shown in Figures 1 and 2 for the normalized bistatic scattering cross section ($\sigma/\pi a^2$) in the E- and H-planes of a sphere with $ka = 60$. Figures 1 and 2 demonstrate that the incremental fields added to the PO fields produce a scattering cross section much closer to that of the exact eigenfunction solution of the sphere than that of the PO solution alone, especially for large bistatic angles. (The exact and PO+ILDC fields are practically indistinguishable over the range of 0 to 90 degrees not shown in Figures 1 and 2.)

The combined work of Yaghjian and Shore in determining shadow-boundary ILDC's was published in 1997 as an invited paper to a special issue of Radio Science on electromagnetic theory [9]. We have been asked by Dr. V. Oliker of MATIS to help implement these shadow-boundary ILDC's in the near future into the production high-frequency computer codes which they continue to develop for the Air Force.

1.3 Surface Integral Equations

In the area of surface integral equations, Yaghjian made substantial progress in 1997 toward solving the problem of the high condition numbers one encounters when applying the electric field integral equation (EFIE) to perfect conductors. These high condition numbers increase the number of required iterations in an iterative solution, and thus they severely limit the size and accuracy obtainable using the EFIE. To quote Professor W.C. Chew from his March 1997 review article in the IEEE Transactions on Antennas and Propagation (Fast Solution Methods in Electromagnetics)

> "Therefore, preconditioning techniques for reducing the required number of iterations in iterative methods are urgently needed in solving electromagnetic wave scattering problems."

Toward this end, Yaghjian was able to determine the root cause of the EFIE condition number increasing with patch density. He also found a very simple, practical preconditioner to stabilize the condition number of the EFIE applied to 2-D scatterers. This preconditioner, which was presented at the 1997 IEEE/URSI International Symposium in Montreal Canada, is presently being tested in the 2-D EFIE computer codes of Boeing-McDonnell Douglas (St. Louis, MO) and Lockheed-Martin (Palmdale, CA).

To understand why and how this EFIE preconditioner works, it helps to begin with the well-conditioned magnetic-field integral equation. Using the theorems on integral equations from [10], it was proven in [11] and confirmed numerically that the spectral condition number for the magnetic-field integral equation (MFIE)

$$\hat{\boldsymbol{n}} \times \boldsymbol{H}_{inc}(\boldsymbol{r}) = -\hat{\boldsymbol{n}} \times \oint_S \mathbf{K}(\boldsymbol{r}') \times \nabla' \psi(\boldsymbol{r}, \boldsymbol{r}') dS' + \frac{\mathbf{K}(\boldsymbol{r})}{2} \tag{12}$$

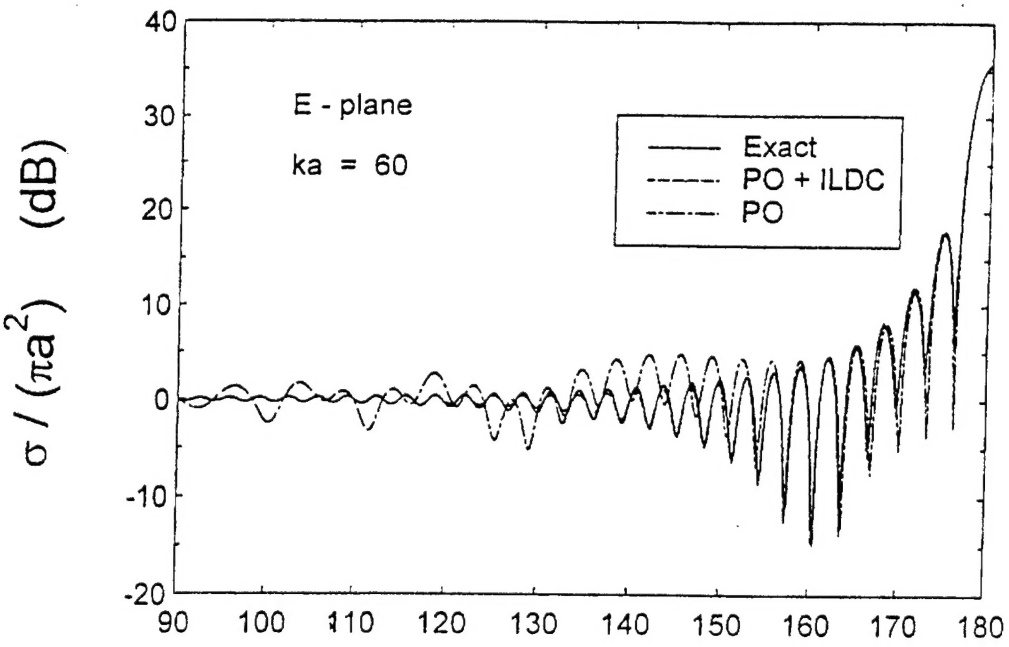

Figure 1: Plot of PO, PO+ILDC, and exact normalized bistatic scattering cross section of a perfectly conducting sphere (E-plane, $ka = 60$).

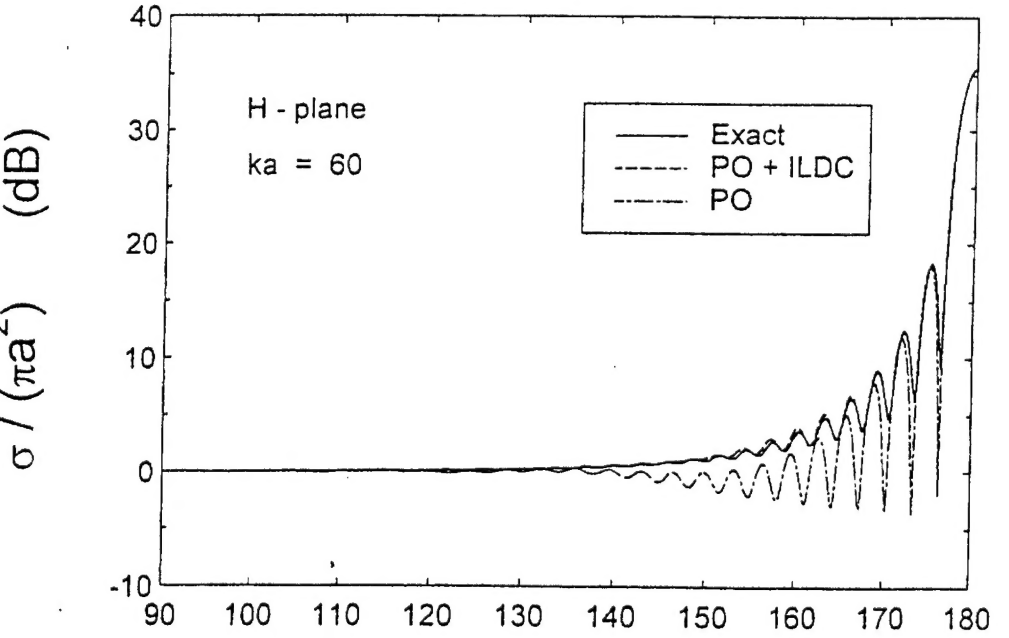

Figure 2: Plot of PO, PO+ILDC, and exact normalized bistatic scattering cross section of a perfectly conducting sphere (H-plane, $ka = 60$).

(modified by a "dual surface" to eliminate spurious resonances [11]) approaches a finite value as the number of patches per square wavelength approaches infinity for a perfectly conducting scatterer of fixed electrical size. Consequently, the number of iterations required to solve the dual-surface MFIE by the conjugate gradient method (or a similar iterative scheme) also approaches a constant as the patch size for a fixed-size scatterer approaches zero [11]. In addition, we found in [11], using pulse basis functions and point matching, that the number of conjugate gradient iterations required to solve for scattering from a cube of surface area A increases as $(A/\lambda^2)^{1/2}$, where λ is the wavelength. Thus, the CPU time required to iteratively solve the MFIE applied to a full-bodied, three-dimensional (3-D) scatterer can be approximated by the proportionality

$$T_M \propto (A/\lambda^2)^{1/2} N^2 \tag{13}$$

where N is the total number of unknowns.

Unlike the MFIE, the conventional electric-field integro-differential equation (EFIE) [12] for the surface current $\mathbf{K}$

$$\hat{\boldsymbol{n}} \times \boldsymbol{E}_{inc}(\boldsymbol{r}) = \frac{1}{i\omega\epsilon} \hat{\boldsymbol{n}} \times \oint_S [k^2 \mathbf{K} \psi(\boldsymbol{r}, \boldsymbol{r}') - (\nabla_s' \cdot \mathbf{K}) \nabla' \psi(\boldsymbol{r}, \boldsymbol{r}')] dS' \tag{14}$$

has a spectral condition number that increases in proportion to the total number of patches per square wavelength for a perfectly conducting scatterer of fixed electrical size [11],[13],[14]. Thus, the total CPU time required to solve the EFIE applied to a 3-D body using an iterative method and a straightforward moment method discretization scheme, will in general be at least as large as

$$T_E \propto (A/\lambda^2)^{1/2} (\lambda^2/\Delta S) N^2 \tag{15}$$

where ΔS is the uniform patch area. For a patch area much smaller than a square wavelength, the CPU time in (15) needed to solve the EFIE iteratively can be much larger than the CPU time in (13) needed to iteratively solve the MFIE. Moreover, the CPU time to iteratively solve the EFIE can quickly become prohibitively large for scatterers that demand finer grid sizes over portions of their surfaces [15].

In 1997 we discovered a convenient preconditioner for 2-D electric-field integral equations that limits the value of the spectral condition number as the patch density increases, thereby reducing the iterative solution time to that given in (13) for the MFIE. Specifically, for a TE and TM plane wave normally incident on a 2-D perfect conductor, (14) can be transformed into

$$\hat{\boldsymbol{n}} \times \boldsymbol{E}_{inc}^{TE}(\boldsymbol{\rho}) = \frac{1}{4\omega\epsilon} \hat{\boldsymbol{n}} \times \left[\oint_C k^2 \mathbf{K}_c H_0^{(1)} dC' + \int_{C-C_\delta} \mathbf{K}_c \cdot \nabla_c' \nabla' H_0^{(1)} dC' \right] - \frac{k H_1^{(1)}(k\delta/2)}{2\omega\epsilon} \hat{\boldsymbol{n}} \times \mathbf{K}_c(\boldsymbol{\rho}) + O(\delta) \tag{16}$$

and

$$E^{TM}_{z,inc} = \frac{k^2}{4\omega\epsilon} \oint_C K_z H_0^{(1)} dC' \tag{17}$$

where $H_0^{(1)}(k|\boldsymbol{\rho} - \boldsymbol{\rho}'|)$ is the Hankel function, $\mathbf{K}_c(\boldsymbol{\rho})$ is the current tangential to the curve defining the boundary of the 2-D scatterer, and δ in (16) is the length of the self-increment C_δ centered on the observation point $\boldsymbol{\rho}$.

We have converted the conventional TE integro-differential equation corresponding to (14) to the pure integral equation in (16) (containing no derivatives of current), in order to allow a clearer comparison with the TE MFIE obtained from (12). Of course, the TM electric-field integral equation in (17) is identical to the conventional TM electric-field integral equation. Its kernel $H_0^{(1)}(k|\boldsymbol{\rho} - \boldsymbol{\rho}'|)$ is less singular than the kernel of the TE electric-field integral equation (16), and it can be solved simply and straightforwardly using, for example, pulse basic functions and point matching. We have also solved the EFIE in (16) for the TE scattering from a 2-D strip using pulse basis functions and point matching. Reasonable accuracy was found for the current using as few as 5 increments per wavelength.

If (14), (16) and (17) are applied to closed perfect conductors, they, like the MFIE in (12), will encounter spurious resonances. For such closed scatterers, these spurious resonances can be eliminated by modifying (14), (16) and (17) with dual surfaces [11], or by combining them with the corresponding MFIE's [16],[17].

Although (14), (16) and (17) can be solved numerically using simple moment methods, all three equations exhibit spectral condition numbers and iterative solution times that increase proportionately with the patch density. If one compares the EFIE's in (14), (16) or (17) with the MFIE in (12) and its 2-D counterparts, which are well-conditioned integral equations, one sees that the significant difference between them, and thus the reason for the ill condition of the EFIE's, is the relatively large values of the kernels within a small fraction of a wavelength from the observation point $\boldsymbol{r}$. In other words, in a MOM representation of (14), (16) or (17) expressed concisely as

$$[Z][K] = [E_{inc}] \tag{18}$$

it is the elements of the impedance matrix Z within a band of about $\lambda/4$ from the diagonal elements that are causing the high condition numbers.

Fortunately, for 2-D problems, this difficulty can be removed through multiplying (18) by the inverse of the banded matrix Z_b formed by keeping only the elements of Z within about $\lambda/4$ of the diagonal elements. Then (18) is transformed to the set of equations

$$[Z_b^{-1}Z][K] = [Z_b^{-1}E_{inc}]. \tag{19}$$

Since Z_b is a matrix banded to about $\lambda/4$, independently of the matrix size, the products $Z_b^{-1}E_{inc}$ and $Z_b^{-1}Z$ can be computed in order N and N^2 operations, respectively. Thus, for multiwavelength bodies, the computer time required to obtain (19) from (18) can be kept

to a small fraction of the total computer time in (13). Moreover, this simple banded-matrix preconditioning converts the matrix representation (18) of the electric-field integral equation (14), (16) or (17) into a matrix representation (19) that is as well conditioned as the MFIE, and that can be solved iteratively in the CPU time T_M given in (13).

These conclusions have been confirmed by solving (18) and (19) iteratively for TE and TM scattering from 2-D strips with widths that varied from one to forty wavelengths. Tables 1 and 2 below show spectral condition numbers and numbers of iterations for the TE scattering. The results for TM scattering are similar but with the number of iterations in the preconditioned cases growing more slowly than the $(\text{stripwidth/wavelength})^{1/2}$ growth exhibited in Table 2 for the TE scattering.

Table 1. TE scattering from 5-wavelength strip

Increments per Wavelength	Number of Iterations without Preconditioning (10^{-6} residual)	Number of Iterations with Preconditioning (10^{-6} residual)
5	22 (5.1)	12 (2.7)
10	48 (11.1)	11 (2.4)
15	72 (16.9)	12 (2.7)
20	96 (22.7)	13 (2.9)
50	did not converge (57.4)	13 (3.0)

(Spectral condition numbers given in parentheses)

Table 2. TE scattering from strips of different widths using 10 increments per wavelength

Strip Width in Wavelengths	Number of Iterations without Preconditioning (10^{-6} residual)	Number of Iterations with Preconditioning (10^{-6} residual)
5	48 (11.1)	11 (2.4)
10	70 (15.3)	14 (3.3)
20	101 (21.3)	21 (4.6)
40	143 (29.8)	30 (6.5)

(Spectral condition numbers given in parentheses)

2 Principal Publications in 1997

Books

1. T.B. Hansen and A.D. Yaghjian, *Plane-Wave Theory of Time-Domain Fields: Application to Near-Field Scanning*, New York: IEEE/Oxford University Press, to appear in 1998.

Book Chapters

1. A.D. Yaghjian and T.B. Hansen, "Theorems on Time-Domain Far Fields," in *Ultra-Wideband, Short-Pulse Electromagnetics 3*, New York: Plenum Press, 1997, 165-176 (Invited).

Journal Articles

1. A.D. Yaghjian, R.A. Shore and M.B. Woodworth, "Shadow-boundary incremental length diffraction coefficients for perfectly conducting smooth, convex surfaces," *Radio Science*, vol. 31, 1681-1695, November-December 1996 (Invited).

2. T.B. Hansen, "Formulation of spherical near-field scanning for time-domain electromagnetic fields," *IEEE Trans. Antennas Propagat.*, vol. 45, 620-630, April 1997.

3. A.N. Norris and T.B. Hansen, "Exact complex source representations of time-harmonic radiation," *Wave Motion*, vol. 25, 127-141, 1997.

4. T.B. Hansen and A.N. Norris, "Exact complex source representations of transient radiation," *Wave Motion*, vol. 25, 1997.

5. A.D. Yaghjian, T.B. Hansen and A.J. Devaney, "Minimum source region for a given far-field pattern," *IEEE Trans. Antennas and Propagat.*, vol. 45, 911-913, May 1997.

6. A.D. Yaghjian, "Banded-matrix preconditioning for electric-field integral equations," *Digest of IEEE Antennas and Propagat. Soc. Int'l Symp. (Montreal Canada)*, vol. 3, 1806-1809, July 1997.

Citations in Science Citation Index

Publications authored and co-authored by Dr. Yaghjian have received an average of 40 citations per year for the past 10 years. In 1996, the last full year of Science Citation Index published to date, his publications received 46 citations. For every author who cites a publication, there are usually many other people who have used that publication in their work but who have not published their work. Thus, this large number of citations each year indicates a considerable transfer of technology.

Appendix A: Derivation of Dispersion Relations

Causality requires that the time-domain constitutive parameters are zero for $t < 0$. We can use this fact to relate the real and imaginary parts of each frequency-domain constitutive parameter by means of the Hilbert transform. Consider, for example, the frequency-domain complex electric susceptibility χ^e_ω, which can be written in terms of the Fourier transform of the time-domain electric susceptibility $\chi^e(t)$ as

$$\chi^e_\omega = \frac{1}{2\pi}\int_0^{+\infty} \chi^e(t)e^{i\omega t}dt = \frac{1}{2\pi}\int_{-\infty}^{+\infty} \frac{t}{|t|}\chi^e(t)e^{i\omega t}dt = \frac{1}{2\pi}\lim_{\delta\to 0}\int_{-\infty}^{+\infty} \frac{t}{|t|}e^{-\delta t}\chi^e(t)e^{i\omega t}dt. \tag{20}$$

The last equality in (20) can be proven valid for $\delta > 0$ using the theorem in [18, vol.2, sec.225] that allows the limit to be brought inside the integral if $\int_{-\infty}^{+\infty} |\chi^e(t)|dt < \infty$. Assume that χ^e_ω is a Hölder continuous function of ω, and for sufficiently large $|\omega|$, $|\chi^e_\omega| \le C/|\omega|^\alpha$, where C and α are positive constants [19, sec.43]. Then one can apply the convolution theorem to the last Fourier transform in (20), use the result

$$\frac{1}{2\pi}\int_{-\infty}^{+\infty} \frac{t}{|t|}e^{-\delta t}e^{i\omega t}dt = \frac{i\omega}{\pi(\omega^2+\delta^2)} \tag{21}$$

rewrite the convolution integral as a Cauchy principal value integral, and take the limit as $\delta \to 0$ (using [18, vol.2, sec.225] and the fact that χ^e_ω is Hölder continuous), to obtain

$$\chi^e_\omega = \frac{i}{\pi}\fint_{-\infty}^{+\infty} \frac{\chi^e_\nu}{\omega-\nu}d\nu \tag{22}$$

where the bar through the integral sign in (22) denotes the Cauchy principal value integration [20, p.368]. Equating the real and imaginary parts of (22), one obtains the "dispersion relations"

$$\chi^{e\prime}_\omega = \frac{1}{\pi}\fint_{-\infty}^{+\infty} \frac{\chi^{e\prime\prime}_\nu}{\nu-\omega}d\nu = \frac{2}{\pi}\fint_0^{+\infty} \frac{\nu\chi^{e\prime\prime}_\nu}{\nu^2-\omega^2}d\nu \tag{23}$$

$$\chi^{e\prime\prime}_\omega = -\frac{1}{\pi}\fint_{-\infty}^{+\infty} \frac{\chi^{e\prime}_\nu}{\nu-\omega}d\nu = -\frac{2\omega}{\pi}\fint_0^{+\infty} \frac{\chi^{e\prime}_\nu}{\nu^2-\omega^2}d\nu. \tag{24}$$

Equations (23)-(24) show that the real and imaginary parts of χ^e_ω are Hilbert transforms of each other [20, p.372]. In fact, these dispersion relations could be obtained directly from the theory of Hilbert transforms, given that the first equation in (20) implies that χ^e_ω is an analytic function in the upper half of the complex ω-plane. Here, however, we have derived the dispersion relations (23)-(24) straightforwardly without relying on the theory of

Hilbert transforms or integrating in the complex ω-plane. In addition, we have determined the conditions on the constitutive parameters, in this case χ^e_ω, that assure the existence of the Hilbert transforms and the validity of the dispersion relations.

The corresponding dispersion relations hold, of course, for the magnetic susceptibility χ^m_ω and conductivity σ_ω, provided they too are Hölder continuous functions of ω that approach zero as $C/|\omega|^\alpha$ or faster ($\alpha > 0$) as $|\omega| \to \infty$. For frequency-domain functions like the complex permittivity $\epsilon_\omega = \epsilon'_\omega + i\epsilon''_\omega = \epsilon(1 + \chi^e_\omega)$, which approaches the free-space value ϵ as $|\omega| \to \infty$, the dispersion relations (23)-(24) can be applied to $(\epsilon_\omega - \epsilon)$ to yield the "Kramers-Kronig dispersion relations" [21, p.311]

$$\epsilon'_\omega - \epsilon = \frac{1}{\pi} \int_{-\infty}^{+\infty} \frac{\epsilon''_\nu}{\nu - \omega} d\nu = \frac{2}{\pi} \int_{-\infty}^{+\infty} \frac{\nu \epsilon''_\nu}{\nu^2 - \omega^2} d\nu \tag{25}$$

$$\epsilon''_\omega = -\frac{1}{\pi} \int_{-\infty}^{+\infty} \frac{\epsilon'_\nu - \epsilon}{\nu - \omega} d\nu = -\frac{2\omega}{\pi} \int_{-\infty}^{+\infty} \frac{\epsilon'_\nu - \epsilon}{\nu^2 - \omega^2} d\nu. \tag{26}$$

Formula (23) (or (25)) is especially useful because approximate values of the odd function $\chi^{e\prime\prime}_\omega$, such that $\chi^{e\prime\prime}_\omega \geq 0$ for $\omega > 0$, can be inserted into (23) to obtain a permissible even function $\chi^{e\prime}_\omega$. However, approximate values of the even function $\chi^{e\prime}_\omega$ inserted into formula (24) may yield an odd function $\chi^{e\prime\prime}_\omega$ that does not satisfy the condition $\chi^{e\prime\prime}_\omega \geq 0$ for $\omega > 0$ [22, p.281].

Each of the dispersion relations (23) and (24) (or (25) and (26)) holds exactly only if the imaginary and real parts, respectively, of the constitutive parameter are known and integrated over all frequencies. Approximate dispersion relations, corresponding to (23) and (24) (or (25) and (26)), can often be found, nonetheless, that produce accurate values of the real and imaginary parts of the constitutive parameter from the local variation of its imaginary and real parts, respectively [23].

Appendix B: Contents of Book Entitled, "Plane-Wave Theory of Time-Domain Fields"

Appendix C: Minimum Source Region for a Given Far-Field Pattern

A number of authors, including[24, th.26] and [25, sec.4.3], have proven that the far-field pattern produced by sources in a volume of finite extent is an entire analytic function of the complex spherical angles (θ, ϕ). In addition, Müller [24, th.26,27,29] has proven that the sources of a given analytic far-field pattern must be contained in a sphere with a radius at least as large as R. The value of R is determined from the spherical expansion coefficients of the far-field pattern, and for many far-field patterns the value of R is greater than zero, regardless of the position of the origin chosen for the spherical expansion. Outside the sphere of radius R, the field of the given analytic far-field pattern is also an analytic function of the spherical coordinates, and this function can be uniquely continued analytically to a minimum source region V_{min} located inside the sphere of radius R. (This can be done, in principle, by expanding the field in a series of Bessel spherical wave functions that converges uniformly up to the surface of the minimum source region [24, ch.3].) Outside V_{min}, which can be singly or multiply connected, the field obeys the homogeneous wave equation. In addition, V_{min} is the smallest possible source region, in that the sources of the given far-field pattern must extend at least as far as the surface of V_{min}, or else the field could be further analytically continued inside the surface.

Here, we derive a simple method, based on the plane-wave spectrum formulation, for determining the minimum convex closed surface S_{min} in which the sources of a given acoustic or electromagnetic far-field pattern can be located, that is, the minimum convex surface enclosing the minimum source region V_{min}. Unlike the value of R in the method based on a spherical wave expansion, the shape and size of S_{min} found here from the plane-wave spectrum is independent of the position of the origin of the coordinate system in which the plane-wave spectrum is defined.

We begin with a result derived in our book, namely, that the far-field functions $F_\omega(k_x, k_y)$ for sources in a volume V of finite extent satisfy the asymptotic relation

$$\lim_{|\gamma|\to\infty} |F_\omega(k_x, k_y)| e^{-|\gamma| z} = 0, \quad z > z_s, \quad \text{for all } k_y/k_x \tag{27}$$

where z_s equals the maximum (more precisely, the supremum) value of z for which the source function $q_\omega(x, y, z)$ is nonzero. Here, z_s can be a negative, zero, or positive real number, depending on the position of the origin of the xyz coordinate system with respect to the source region.

An infinite number of different source distributions can radiate the same far field, and thus produce the same field everywhere outside the source region. For example, any number of spherically symmetric source distributions produce the same constant far-field pattern. Thus, depending on the particular source distribution $q_\omega(x, y, z)$, (27) may hold for $z > z_1$ with $z_1 < z_s$. Moreover, unless the source distribution can be zero everywhere (and thus

not radiate at all), there must be a minimum z_1 for which the limit in (27) is zero. Letting z_{min} be the maximum value that z attains in V_{min}, so that $z \leq z_{min}$ when $\boldsymbol{r} \in V_{min}$, the minimum z_1 is equal to z_{min}. To prove this, assume that z_1 were less than z_{min}, so that the plane $z = z_1$ cuts through the minimum source region V_{min}. Then the spectrum $T_\omega(k_x, k_y) = (i/\gamma)F_\omega(k_x, k_y)$ would decay exponentially according to (27) for $z > z_1$, and the field given by the plane-wave expansion

$$p_\omega(\boldsymbol{r}) = \frac{1}{2\pi} \int_{-\infty}^{+\infty} \int_{-\infty}^{+\infty} T_\omega(k_x, k_y) e^{i(k_x x + k_y y + \gamma z)} dk_x dk_y \tag{28}$$

would satisfy the homogeneous wave equation for $z > z_1$ and be an analytic function of the spatial coordinates for $z > z_1$.[1] Consequently, $z = z_1$ cannot cut through the minimum source region, and the minimum value of z_1 is therefore equal to z_{min}.

Hence, for $z < z_{min}$, the limit in (27) is indeed not equal to zero at least for one value of k_y/k_x as $|\gamma| = |k_x^2 + k_y^2 - k^2|^{1/2} \to \infty$, so for any far-field function generated by sources in a volume of finite extent, we have

$$\limsup_{|\gamma| \to \infty} |F_\omega(k_x, k_y)| e^{-|\gamma| z} = \begin{cases} 0, & z > z_{min}, \quad \text{for all } k_y/k_x \\ \infty, & z < z_{min}, \quad \text{for at least one } k_y/k_x. \end{cases} \tag{29}$$

The infinite value occurs on the lower right side of (29) because if the value of the limit is nonzero for all $z < z_{min}$, the exponential factor on the left side of (29) demands that its value be infinite for all $z < z_{min}$. The "limit superior" [27, p.68] is necessary in (29) to allow for oscillating values of $F_\omega(k_x, k_y)$ as $|\gamma| \to \infty$.

The condition (29) can be rewritten as follows in terms of a far-field pattern $\mathcal{F}_\omega(\theta, \phi)$

$$\limsup_{\theta \to \frac{\pi}{2} - i\infty} |\mathcal{F}_\omega(\theta, \phi)| e^{-kz|\cos\theta|} = \begin{cases} 0, & z > z_{min}, \quad \text{for all } \phi \\ \infty, & z < z_{min}, \quad \text{for at least one } \phi\,. \end{cases} \tag{30}$$

where we have used the fact that

$$\mathcal{F}_\omega(\theta, \phi) = F_\omega(k \cos\phi \sin\theta, k \sin\phi \sin\theta) \tag{31}$$

for $0 \leq \phi \leq 2\pi$; $0 \leq \theta \leq \pi/2$ and $\theta = \pi/2 - i\alpha$ with $0 \leq \alpha < \infty$.

Now, suppose we are given an analytic far-field pattern and have determined the value of z_{min} such that (30) is satisfied. The minimum source region V_{min} for this far-field pattern must extend in the z direction as far as $z = z_{min}$. If (30) holds for all orientations of the z axis

[1] To prove that the field in (28) satisfies the homogeneous wave equation for $z > z_1$, apply the ∇^2 operator to the right side of (28) and interchange the integrations and differentiations for $z > z_1$ as allowed by the exponential decay of the integrand [26, sec.6.2.3]. Similarly, it follows that the field in (28) is an analytic function of x, y, and z in domains that include the real x, y, and z axes.

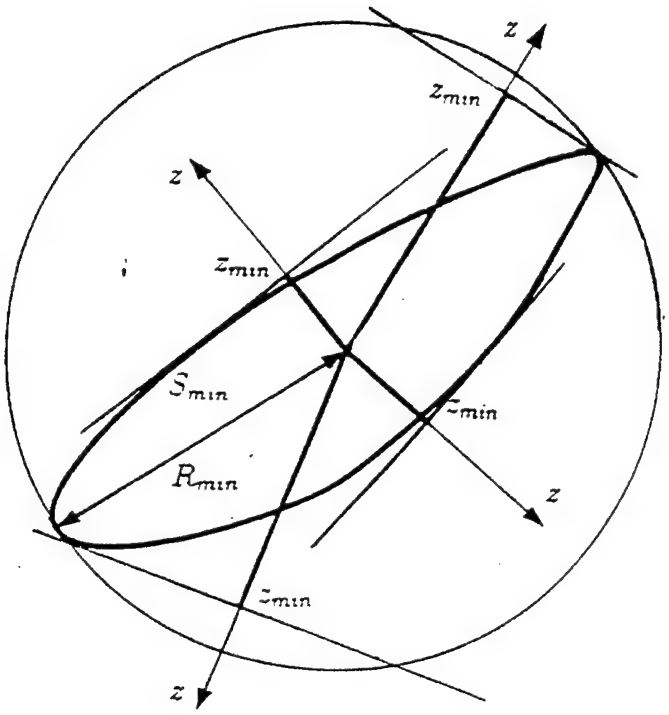

Figure 3: Minimum convex closed surface S_{min} formed by the locus of points z_{min} for all orientations of the z axis.

(with z_{min} and $\mathcal{F}_\omega(\theta,\phi)$ depending, in general, on the orientation), then the corresponding spectrum $T_\omega(k_x,k_y)$ for all orientations of the z axis can be inserted into (28) to generate a function $p_\omega(\boldsymbol{r})$ that satisfies the homogeneous wave equation outside the minimum convex closed surface S_{min} formed by all the z_{min}, as shown in Figure 3. In other words, S_{min} will be the minimum convex surface enclosing the minimum source region. The plane-wave representation (28) also gives us the value of $p_\omega(\boldsymbol{r})$ and all its derivatives on S_{min}. In particular, it gives the Huygens' sources ($p_\omega(\boldsymbol{r})$ and $(\partial/\partial n)p_\omega(\boldsymbol{r})$) that generate the fields outside S_{min}.

Consequently, we have proven that a far field satisfying the conditions (29) or (30) for every orientation of the z axis can be generated by sources that lie within or on the minimum convex closed surface S_{min} determined by the locus of values of z_{min} for all orientations of the z axis. Moreover, this far field cannot be generated by sources that extend to a radius that is less than the radius R_{min} of the sphere that circumscribes S_{min} (see Figure 3). If the origin of this circumscribing sphere is chosen as the origin of the coordinate system that Müller [24] uses to expand the fields in spherical waves, then this R_{min} equals the minimum R in [24, th.26,27]. For other origins, Müller's minimum R is greater than R_{min}. Of course, the sources that generate the far-field pattern $\mathcal{F}_\omega(\theta,\phi)$ are not unique and can be chosen to extend outside S_{min}.

For many far-field patterns, S_{min} will simply be a single point in space so that $R_{min} = 0$. This means that the pressure $p_\omega(\boldsymbol{r})$ associated with $\mathcal{F}_\omega(\theta, \phi)$ can be produced by a convergent sum of spherical multipoles located at a single point in space (S_{min}). If $R_{min} > 0$, a multipole expansion (located at the center of the sphere with radius R_{min}) of the pressure $p_\omega(\boldsymbol{r})$ having the far-field pattern $\mathcal{F}_\omega(\theta, \phi)$ will converge for radii $r > R_{min}$. Moreover, at least for some spherical angles (θ, ϕ), it will diverge when $r < R_{min}$. If the infinite sum of spherical multipoles is truncated to a finite mode number N, the resulting approximate field will converge, of course, for all $r > 0$ but will have extremely high reactive fields for $r < N/k$ [28],[29].

For electromagnetic fields, the scalar acoustic far field is merely replaced by the vector electromagnetic far field, and (29) and (30) are replaced by

$$\limsup_{|\gamma|\to\infty} |\mathbf{F}_\omega(k_x, k_y)| e^{-|\gamma| z} = \begin{cases} 0, & z > z_{min}, \quad \text{for all } k_y/k_x \\ \infty, & z < z_{min}, \quad \text{for at least one } k_y/k_x \end{cases} \tag{32}$$

$$\limsup_{\theta\to\frac{\pi}{2}-i\infty} |\mathcal{F}_\omega(\theta, \phi)| e^{-kz|\cos\theta|} = \begin{cases} 0, & z > z_{min}, \quad \text{for all } \phi \\ \infty, & z < z_{min}, \quad \text{for at least one } \phi\,. \end{cases} \tag{33}$$

Example

We shall now use of the acoustic formula (30) to determine the minimum convex surface S_{min} for the far-field pattern of a circular-disk acoustic radiator of radius a. This far-field pattern as a function of spherical angles (θ, ϕ) measured with respect to a rectangular xyz coordinate system, with z axis normal to the circular disk and passing through the center of the disk at $z = 0$, is given by

$$\mathcal{F}_\omega(\theta, \phi) = A \frac{J_1(ka \sin\theta)}{\sin\theta}\,, \quad 0 \le \theta \le \pi \tag{34}$$

where $J_1(x)$ is the first order Bessel function, and A is a constant independent of θ and ϕ. For this particular orientation of the z axis, the far-field pattern is independent of the azimuthal angle ϕ.

Substituting the far-field pattern (34) into (30) shows that $z_{min} = 0$ for this z axis normal to the center of the disk. For the z axis pointed in the opposite direction, z_{min} also equals zero, because $\sin(\pi - \theta) = \sin\theta$; that is, the far-field pattern in (34) is identical to the right and left of the circular-disk radiator. Thus, we have confirmed that the sources of the far-field pattern (34) can all lie in the plane of the circular disk that radiates this far-field pattern.

To find the minimum distance that the sources must extend from the center of the disk in a direction in the plane of the disk, rotate the z axis 90° about the y axis and rewrite the far-field pattern in terms of the new spherical angles (θ', ϕ') measured with

respect to this rotated z axis, which now lies in the plane of the disk. Specifically, we have $\sin\theta = (1 - \sin^2\theta' \cos^2\phi')^{1/2}$ and (34) shows that

$$\mathcal{F}_\omega(\pi/2 - i\alpha, \phi') = A \frac{J_1\left(ka\sqrt{1 - \cosh^2\alpha \cos^2\phi'}\right)}{\sqrt{1 - \cosh^2\alpha \cos^2\phi'}}, \quad 0 \le \alpha < \infty \tag{35}$$

where we have also used $\sin(\pi/2 - i\alpha) = \cosh\alpha$. Since

$$(1 - \cosh^2\alpha \cos^2\phi')^{1/2} \sim \pm i |\cos\phi'| \cosh\alpha, \qquad \alpha \to \infty, \qquad \cos\phi' \neq 0 \tag{36}$$

the asymptotic formula

$$\frac{J_1(\pm ix)}{\pm ix} \sim \frac{e^x}{x\sqrt{2\pi x}}, \qquad x \to \infty \tag{37}$$

can be invoked to get

$$\limsup_{\alpha\to\infty} |\mathcal{F}_\omega(\pi/2 - i\alpha, \phi')| e^{-kz\sinh\alpha} = \limsup_{\alpha\to\infty} \frac{A\, e^{ka\cosh\alpha|\cos\phi'|}\, e^{-kz\sinh\alpha}}{\sqrt{2\pi ka}\,(\cosh\alpha|\cos\phi'|)^{3/2}} \tag{38}$$

when $\cos\phi' \neq 0$. For $\cos\phi' = 0$, we have $\mathcal{F}_\omega(\pi/2 - i\alpha, \phi') = A\, J_1(ka)$. Combining these results shows that

$$\limsup_{\theta'\to\frac{\pi}{2}-i\infty} |\mathcal{F}_\omega(\theta', \phi')| e^{-kz|\cos\theta'|} = \begin{cases} 0, & z > a, \quad \text{for all } \phi' \\ \infty, & z < a, \quad \text{for at least one } \phi'. \end{cases} \tag{39}$$

Comparing (39) with (30), we see that $z_{min} = a$ for any orientation of the z axis in the plane of the disk. Therefore, the minimum convex surface S_{min} containing sources that can produce the far-field pattern of the circular-disk radiator simply coincides with the actual infinitesimally thin physical disk of radius a. Of course, the same far-field pattern could be excited by sources that extend outside this disk. However, the above exercise has proven that the physical disk comprising the circular acoustic radiator is the smallest source region that can exactly produce its far-field pattern.

In summary, when an exact closed form expression for the acoustic far field is known, (29), or equivalently (30), determines the minimum convex closed surface in which the sources of the far field can reside.

References

[1] T.B. Hansen and A.D. Yaghjian, "Planar near-field scanning in the time domain, Parts 1 & 2: Formulation & Sampling theorems and computation schemes," *IEEE Trans. Antenna Propagat.*, vol. AP-42, 1280-1300, September 1994.

[2] T.B. Hansen and A.D. Yaghjian, *Plane-Wave Theory of Time-Domain Fields: Application to Near-Field Scanning*, New York: IEEE/OUP, to appear in 1998.

[3] A.D. Yaghjian and T.B. Hansen, "Theorems on Time-Domain Far Fields," in *Ultra-Wideband, Short-Pulse Electromagnetics 3*, New York: Plenum Press, 1997, 165-176.

[4] A.D. Yaghjian, T.B. Hansen and A.J. Devaney, "Minimum source region for a given far-field pattern," *IEEE Trans. Antennas and Propagat.*, vol. 45, 911-913, May 1997.

[5] A.D. Yaghjian (1992) *Relativistic Dynamics of a Charged Sphere: Updating the Lorentz-Abraham Model*, New York: Springer-Verlag.

[6] R.A. Shore and A.D. Yaghjian, "Incremental diffraction coefficients for planar surfaces," *IEEE Trans. Antennas Propagat.*, vol. 36, 55-70, January 1988.

[7] R.A. Shore and A.D. Yaghjian, "Application of incremental length diffraction coefficients to calculate the pattern effects of the rim and surface cracks of a reflector antenna," *IEEE Trans. Antennas Propagat.*, vol. 41, 1-11, January 1993.

[8] P.M. Johansen, "Uniform physical theory of diffraction equivalent edge currents for truncated wedge strips," *IEEE Trans. Antennas Propagat.*, vol. 44, 989-995, July 1996.

[9] A.D. Yaghjian, R.A. Shore and M.B. Woodworth, "Shadow-boundary incremental length diffraction coefficients for perfectly conducting smooth, convex surfaces," *Radio Science*, vol. 31, 1681-1695, November-December 1996; Correction, vol. 32, 673, March-April 1997.

[10] R. Courant and D. Hilbert, *Methods of Mathematical Physics*, New York:Interscience, 1953, vol. 1, ch.3.

[11] M.B. Woodworth and A.D. Yaghjian, "Multiwavelength three-dimensional scattering with dual-surface integral equations," *J. Opt. Soc. Am. (A)*, vol. 11, 1399-1413, 1994.

[12] A.J. Poggio and E.K. Miller, "Integral equation solutions of three-dimensional scattering problems," ch.4 of *Computer Techniques for Electromagnetics*, Ed. R. Mittra, Oxford:Pergamon, 1973.

[13] L.M. Correia, "A comparison of integral equations with unique solution in the resonance region for scattering by conducting bodies," *IEEE Trans. Antennas Propagat.*, vol. 41, 52-58, 1993.

[14] F.X. Canning, "Diagonal preconditioners for the EFIE using a wavelet basis," *IEEE Trans. Antennas Propagat.*, vol. 44, 1239-1246, 1996.

[15] C. Lu, W.C. Chew and J. Song, "A study of disparate grid sizes for an irregular-shape scatterer on EFIE, MFIE, and CFIE," *Digest of IEEE AP-S Int. Symp.*, Baltimore, MD, July 1996, 1746-1749.

[16] J.R. Mautz and R.F. Harrington, "H-field, E-field, and combined-field solutions for conducting bodies of revolution," *AEC*, vol. 32, 157-164, 1978.

[17] A.D. Yaghjian, "Augmented electric- and magnetic-field integral equations," *Radio Science*, vol. 16, 987-1001, 1981.

[18] E.W. Hobson, *The Theory of Functions of a Real Variable*, NY: Dover, Vol. II, 1957.

[19] N.I. Muskhelishvili, *Singular Integral Equations*, Groningen-Holland: Noordhoff, 1953.

[20] P.M. Morse and H. Feshbach, *Methods of Theoretical Physics*, New York: McGraw-Hill, Part I, 1953.

[21] J.D. Jackson, *Classical Electrodynamics*, 2nd edition, New York: Wiley, 1975.

[22] L.D. Landau, E.M. Lifshitz, and L.P. Pitaevskii, *Electrodynamics of Continuous Media*, 2nd edition, New York: Pergamon Press, 1984.

[23] M. O'Donnell, E.T. Jaynes and J.G. Miller, "General relationships between ultrasonic attenuation and dispersion," *J. Acoust. Soc. Am.*, vol. 63, 1935-1937.

[24] C. Müller, *Foundations of the Mathematical Theory of Electromagnetic Waves*, New York: Springer-Verlag, 1969.

[25] M. Nieto-Vesperinas, *Scattering and Diffraction in Physical Optics*, NY: Wiley, 1991.

[26] W. Kaplan, *Advanced Calculus*, 4th edition, Reading, MA: Addison-Wesley, 1991.

[27] J.M.H. Olmsted, *Real Variables*, New York: Appleton-Century-Crofts, 1959.

[28] L.J. Chu, "Physical limitations of omni-directional antennas," *J. Appl. Phys.*, vol. 19, 1163-1175, December 1948.

[29] A.D. Yaghjian, "Sampling criteria for resonant antennas and scatterers," *J. Appl. Phys.*, vol. 79, 7474-7482, May 1996.

REPORT DOCUMENTATION PAGE

AFRL-SR-BL-TR-00-

0408

ources,
of this
fferson

1. AGENCY USE ONLY *(Leave blank)*	2. REPORT DATE	3. RE
		10 April 1997 - 30 December 1997

4. TITLE AND SUBTITLE
Research in Electromagnetic Scattering

5. FUNDING NUMBERS
F49620-97-C-0017

6. AUTHOR(S)
Dr. Arthur Yaghjian

7. PERFORMING ORGANIZATION NAME(S) AND ADDRESS(ES)
A.J. Devaney Associates, Inc.
295 Huntington Avenue, Suite 208
Boston, MA 02115

8. PERFORMING ORGANIZATION REPORT NUMBER

9. SPONSORING/MONITORING AGENCY NAME(S) AND ADDRESS(ES)
AFOSR
801 North Randolph Street, Room 732
Arlington, VA 22203-1977

10. SPONSORING/MONITORING AGENCY REPORT NUMBER
F49620-97-C-0017

11. SUPPLEMENTARY NOTES

12a. DISTRIBUTION AVAILABILITY STATEMENT
Approved for Public Release.

12b. DISTRIBUTION CODE

13. ABSTRACT *(Maximum 200 words)*

The document constitutes a final report for our research in electromagnetic scattering during 1997. The technical research accomplishments divided conveniently into the areas of time-domain electromagnetic, high-frequency diffraction, and surface integral equations. As principal invesgator, Dr. Arthur D. Haghjian carried out the major portion of the research, and coordinated his efforts with those of T.B Hansen and R.A. Shore of Rome Laboratory, R. A. Albanese of Brooks AFB, S.W. Lee of DEMAC, and R. Tolimieri, M An and A.J. Devaney of A. J. Devaney Associates.

14. SUBJECT TERMS	15. NUMBER OF PAGES
	25
	16. PRICE CODE

17. SECURITY CLASSIFICATION OF REPORT	18. SECURITY CLASSIFICATION OF THIS PAGE	19. SECURITY CLASSIFICATION OF ABSTRACT	20. LIMITATION OF ABSTRACT